Journal of Power Sources 248 (2014) 489–497

Contents lists available at ScienceDirect

Journal of Power Sources

journal homepage: www.elsevier.com/locate/jpowsour

Neutron depth profiling of Li-ion cell electrodes with a gas-controlled environment

Shrikant C. Nagpure [a,c,*], Padhraic Mulligan [b,c], Marcello Canova [a,c], Lei R. Cao [b,c]

[a] Center for Automotive Research, Ohio State University, Columbus, OH 43212, USA
[b] Nuclear Engineering Program, Department of Mechanical and Aerospace Engineering, Ohio State University, Columbus, OH 43210, USA
[c] Department of Mechanical and Aerospace Engineering, Ohio State University, Columbus, OH 43210, USA

HIGHLIGHTS

- Measurement of lithium concentration with neutron depth profiling (NDP) in electrodes of aged commercial Li-ion batteries.
- Demonstration of a modified NDP facility with a gas-controlled environment for air-sensitive Li-ion battery samples.
- Evaluation of measurement of lithium concentration during the operation of the Li-ion cell containing a liquid electrolyte.
- Monte-Carlo simulations to optimize the pressure of the inert gas in the NDP chamber for high measurement accuracy.

ARTICLE INFO

Article history:
Received 14 June 2013
Received in revised form
25 August 2013
Accepted 6 September 2013
Available online 5 October 2013

Keywords:
Li-ion batteries
Lithium concentration
Measurement techniques
Neutron depth profiling

ABSTRACT

Neutron depth profiling (NDP) is a nondestructive technique that has been applied to characterize the lithium concentration in the electrode materials of Li-ion batteries as a function of depth. NDP measurements have been traditionally performed ex-situ, under vacuum of the order of 10^{-6} Torr to avoid any change in the residual energy of the charged particles as they emerge from the sample surface. In this work, we describe the design of the NDP measurement facility that allows for conducting tests at variable pressure conditions, through an inert gas atmosphere. This study enhances the ability of the conventional NDP instrument to measure lithium concentration of air-sensitive materials without exposure to atmospheric conditions and under inert gas atmosphere. Furthermore, it provides the opportunity to conduct in-situ NDP on Li-ion cells using liquid electrolytes that would otherwise evaporate at high vacuum conditions.

1. Introduction

Lithium ion batteries are the energy storage technology that has enabled the commercialization of electric and plug-in hybrid vehicles. This advanced battery technology has emerged over other chemistries due to its high energy and power density, excellent rate capabilities and safe operation under various environmental and operating conditions [1]. Nevertheless, the commercial success of electric and plug-in hybrid electric vehicles will ultimately depend on the ability of the battery to retain performance and reliability after many usage cycles. While the operation of Li-ion batteries is well understood, considerable research effort is today focused on understanding the mechanisms and fundamental causes that lead to the aging and degradation of the battery materials. To this extent, several measurement and characterization techniques have been adopted (and in some case developed) to analyze the effects of degradation mechanisms on the morphological and electrochemical properties of Li-ion battery materials [2,3]. It is well understood that measuring or predicting the lithium concentration within the electrodes or electrolyte solution is the key to characterize the transport and electrochemical reactions that occur during the charging and discharging process of a cell. This is particularly critical for the operation of aged Li-ion batteries, where several complex physiochemical phenomena affect the intercalation/deintercalation mechanisms and the transport in solid and liquid phase, ultimately resulting in loss of capacity and power.

However, developing quantitative and direct measurement methods characterizing the lithium concentration within a sample has been extremely challenging. For instance, electron-based techniques such as energy dispersive X-ray spectroscopy (EDS) or electron energy loss spectroscopy (EELS) have been used in the past to measure the lithium bonding with its neighboring atoms in the

* Corresponding author. Center for Automotive Research, Ohio State University, Columbus, OH 43212, USA.
E-mail address: nagpure.1@osu.edu (S.C. Nagpure).

0378-7753/$ – see front matter © 2013 Elsevier B.V. All rights reserved.
http://dx.doi.org/10.1016/j.jpowsour.2013.09.032

structure of electrode materials [2]. Unfortunately, electron based techniques fail to detect light elements (such as lithium) because of the low energy of the X-rays emitted from light elements, which can not escape the beryllium window on the EDS or EELS detector systems. Thus direct measurement of lithium concentration is difficult with electron-based techniques.

On the other hand, neutrons have high penetration power for most of the elements but is almost opaque to light elements such as lithium. Exploiting the interaction of neutrons with lithium, several techniques have been applied to study the structure of Li-ion electrode materials, including neutron diffraction, radiography, imaging and small angle scattering [4].

Among others, Neutron Depth Profiling (NDP) is a nondestructive technique that is able to provide a quantitative measure of the concentration profiles of lithium within the host material, as a function of the thickness of the sample. Ziegler et al. [5] was the first to use a nuclear reaction experiment to determine the concentration of boron impurities in silicon wafers. The sample was bombarded with a well-collimated beam of low energy neutrons in vacuum, and the emitted energized particles were analyzed using a charged-particle spectroscopy for the concentration profile of the ^{10}B in the sample. Later, Downing et al. [6,7] and Biersack et al. [8] used this technique extensively to measure the concentration profiles of other neutron sensitive light-weight isotopes.

More recently, Whitney et al. [9] and Nagpure et al. [10,11] have demonstrated the application of NDP to measure the lithium concentration in the near surface region of commercial Li-ion battery materials, providing a wealth of information on the effects of degradation on the lithium concentration profiles in cathode and anode electrodes. Recently, in-situ neutron depth profiling experiments have been conducted to provide a measurement of lithium concentration in the electrodes during utilization of the cell. For instance, Oudenhoven et al. [12] have used NDP for in-situ characterization using an all solid state Li-ion cell tested under vacuum conditions. The need to establish a vacuum environment during the measurement process limits considerably the options for designing in-situ Li-ion cells, particularly preventing the use of liquid electrolytes that are common in commercial cells. In fact, the conventional alkylene-based electrolytes do not have suitable vapor pressure (Table 1) if the in-situ studies are to be conducted in vacuum [13].

This work attempts to overcome the aforementioned limitations by proposing a novel NDP experimental setup that allows one to prepare and conduct tests in a controlled inert gas atmosphere.

This paper aims at benchmarking the ability of the OSU-NDP instrument to measure the lithium concentration profiles in the near-surface region of commercial electrodes. To this extent, several samples of cathode and anode materials were harvested from samples of commercial Li-ion batteries, both new and aged after accelerated cycling. The benchmarking was conducted by comparing the results to experimental tests previously conducted at the NDP facility at the National Institute of Standards and Technology (NIST) [10]. Furthermore, a preliminary evaluation was conducted to verify the ability of the OSU-NDP facility to measure the Li-ion concentration under an inert gas environment at ambient pressure conditions. Based on the preliminary experimental results, Monte-Carlo simulations were conducted to determine how the inert gas affects the measurement accuracy at different pressures, establishing a trade-off between system pressure and measurement accuracy. The paper is structured as follows. First, a discussion of the NDP operating principles and the required signal processing to measure the lithium concentration is presented. Then, the OSU-NDP facility fitted with the new design implementations is discussed. The benchmarking of ex-situ OSU-NDP (on dry samples) is then conducted to evaluate the accuracy of the instrument. Finally, a description of how the pressure of inert gas in the chamber affects the instrument accuracy and range in measuring the Li-ion concentration based on experimental and simulation data is discussed.

2. The basic principles of NDP

The NDP technique is based on the energy release of nuclear reactions between certain light elements and the incident neutrons. The counts and the residual energy of the charged particles generated in this reaction are used to generate the concentration profile of the sampled element. When a sample is irradiated with a well collimated beam of thermal or cold neutrons, isotopes such as ^{6}Li, ^{3}He, ^{10}B etc. undergo an exoergic charged particle reaction. Based on the reacting element either a proton or an alpha particle and a recoiling nucleus are generated. Using the *Q-value* of the reaction the energies of the emitted particles can be determined and the element can be identified. In Li-ion battery samples, the reaction proceeds as:

$$^{6}\mathrm{Li} + \mathrm{n} \rightarrow {}^{4}\mathrm{He}\ (2055\ \mathrm{keV}) + {}^{3}\mathrm{H}\ (2727\ \mathrm{keV}) \quad (1)$$

When a sample is illuminated with a beam of low energy neutrons ($<10^{-2}$ eV) uniformly, most of the neutrons pass through the sample without any interference (Fig. 1). At some sites within the sample the reacting atoms capture the neutrons based on their reaction cross-section and generate monoenergetically charged particles. The isotropically emitted charged particle and recoil nucleus lose energy via mainly electronic interactions while travelling through the sample host material. Since both the sample and charged particle detectors are housed in vacuum, the particles do not lose energy after emerging from the sample surface. By measuring the residual energy of charged particles, the path length of the charged particles from the reaction site can be determined using the material's stopping power and the equation

$$x = \int_{E(x)}^{E_0} dE/S(E) \quad (2)$$

where x is the path length, E_0 is the particle's initial energy, $E(x)$ is the residual energy after leaving the sample, and $S(E)$ is the stopping power of the sample material. The stopping power of the sample material can be determined using the stopping and range of ions in matter (SRIM) code of Ziegler et al. [14]. By measuring the number of particles traversing a given path length, the concentration of that parent isotope can be determined for a known neutron flux and detector efficiency or by way of comparison to a certified standard material.

3. Description of the OSU-NDP setup

3.1. Experimental set-up

Fig. 2 shows the OSU-NDP chamber as described in Ref. [15]. The vacuum chamber is a 61 cm × 61 cm right circular cylinder made of stainless steel 304, connected to a turbomolecular vacuum pump able to reach an operating pressure below 10^{-6} Torr. The neutron beam enters and exits the chamber through 80 μm thin aluminum windows. The charged particles are detected by an array of 8 silicon

Table 1
Liquid electrolyte vapor pressure [13].

Solvent (formula)	Vapor pressure (Pa)
Ethylene carbonate ($C_3H_4O_3$)	1.33 (20 °C)
Propylene carbonate ($C_4H_6O_3$)	4 (25 °C)
Dimethyl carbonate ($C_3H_6O_3$)	5300 (20 °C)
Diethyl carbonate ($C_5H_{10}O_3$)	1400 (25 °C)

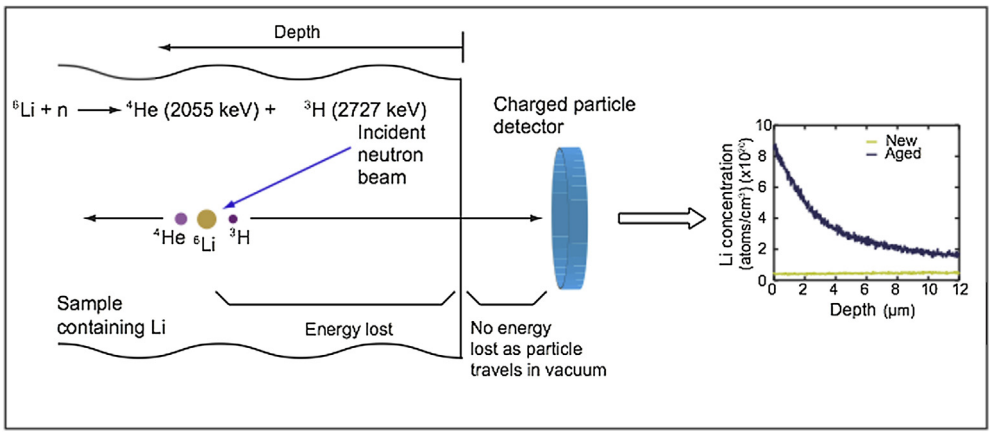

Fig. 1. Overview of the principles of NDP measurement method.

charged particle detectors, arranged annularly around the front entrance window. A set of Ortec ULTRA™, boron-implanted silicon detectors with a 300 mm^2 active surface area and 100 μm depletion depth are used. The detectors can be individually arranged such that the angle between the detector and the sample can be varied from approximately from 20° to 90°. The samples are mounted on an aluminum disk centered in the neutron beam.

3.2. Description of the system modification

The NDP system described above was designed for ex-situ measurements in vacuum, without consideration of environment control. Due to the unique requirement of an inert atmosphere while handling Li-ion battery electrode samples, as well as for enabling in-situ measurements, a set of modifications was applied to the NDP instrument.

A two-gas system was built for safe handling of the samples and to create an inert gas environment during the NDP experiments. Specifically, an inert gas environment around the NDP chamber was built to serve as an intermediate sample handling/loading chamber. As can be seen in Fig. 3, a plastic glove bag is fixed around the opening of the NDP chamber that serves as an intermediate sample holding chamber. Both gas cylinders are connected to a regulator with flowmeter to control the flow of the gas through the chamber (Fig. 4). The two gas lines are then connected to a 3-way isolation valve, so that only one of the gases is introduced to the chamber at a time. The 3-way connector is then connected to an inlet port on the NDP chamber.

The test sample (air sensitive) is brought to the NDP facility in a sealed inert gas container and placed in the glove bag with the NDP chamber cover unlocked. The system is then evacuated with the pump. Once an acceptable level of vacuum is reached the system is back filled with the argon gas. This incoming inert gas also inflates the glove bag and creates an inert atmosphere within the glove bag. The samples are then taken out from their sealed container and loaded on the NDP sample mount. The NDP chamber is then evacuated, removing the argon gas, to the operating vacuum

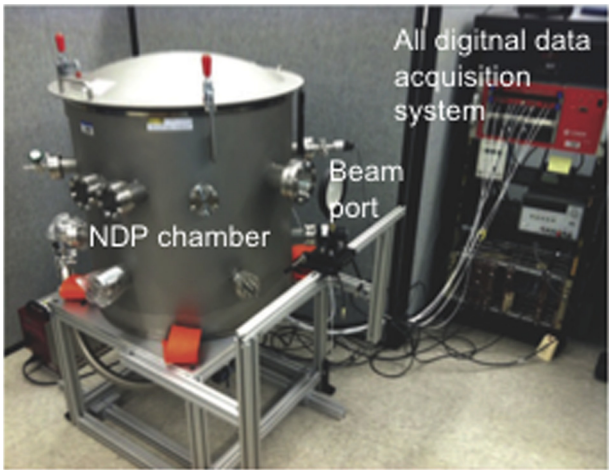

Fig. 2. Overview of the OSU-NDP facility.

Fig. 3. Modified OSU-NDP facility with a glove bag for intermediate holding of samples in inert atmosphere.

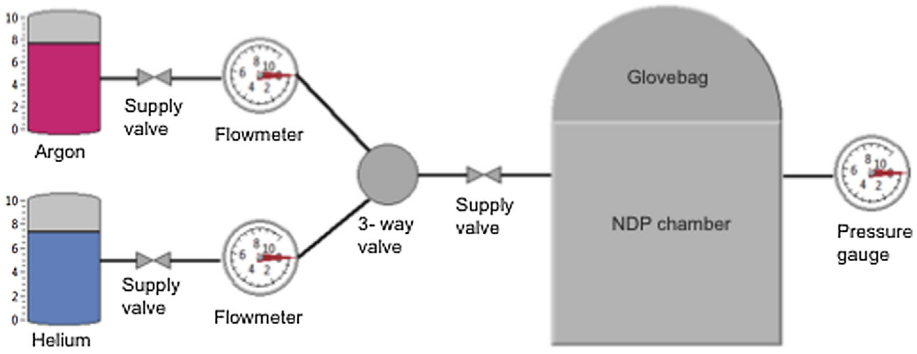

Fig. 4. The gas system to create the inert atmosphere for loading/unloading of samples and conducting NDP experiment in inert atmosphere at 1 atm pressure.

pressure of 10^{-6} Torr. The test proceeds with NDP measurement if vacuum is acceptable. If the test needs to be conducted in an inert gas atmosphere, then the chamber is back filled with helium gas until the pressure within the NDP chamber is slightly below 1 atm.

4. Description of the NDP experiments and results

4.1. Sample preparation

A set of experiments was conducted on samples of electrode materials harvested from secondary lithium-ion cells to benchmark the modified OUS-NDP facility against the NIST facility. The samples were extracted from commercial cylindrical cells (26,650 size) with nominal capacity of 2.3 Ah and nominal voltage of 3 V. The electrolyte in these commercial cells is $LiPF_6$ in a 1:1 mixture of ethylene carbonate (EC) and dimethyl carbonate (DMC). The graphite negative electrode is bonded onto a copper substrate, while the cathode is formed by a porous layer of $LiFePO_4$ nanoparticles (40–50 nm thickness) bonded onto an aluminum substrate using a polyvinylidene difluoride (PVDF) binder. In order to improve the poor electronic conductivity of $LiFePO_4$ ($\sigma = 2 \times 10^{-9}$ S cm^{-1} according to [16]), the nanoparticles are coated with carbon.

The cells were subjected to accelerated aging, through the application of a periodic current profile generated from the analysis of experimental data from fleets of electric and hybrid electric vehicles. In particular, Table 2 summarizes the different testing protocols adopted in the aging study. A thorough description of the testing campaign and results is reported in Refs. [17,18]. For the benchmarking study, samples were obtained by harvesting cathode and anode materials from this set of cells that have been previously characterized at NIST.

Four cells were made available for harvesting the electrodes that were used in these experiments. The cell named C0 in Table 2 refers to a cell that was characterized at the beginning of life (BOL) to establish a baseline condition for comparison of performance and lithium concentration profiles for the aged cells. The cells C2 and C4 were cycled using a time-varying current profile designed to maintain the State of Charge (SOC) in a range from 0% to 10%, with a C-rate of 2C and 4C, respectively (1C-rate = 2.3 Ah), and temperature at 55 °C. These tests, as reported in Refs. [19–21], were representative of limiting conditions for the operation of Li-ion battery packs for Plug-in Hybrid Electric Vehicles (PHEV). Finally, the cell C7 was aged by imposing current cycles forcing the cell to operate in a SOC range from 68% to 75% with a variable C-rate (up to7C) at 45 °C, to represent operating conditions typical for a charge-sustaining HEV.

Table 2
Details of the aging conditions for the cells from which the anode and the cathode samples were harvested.

Cells	C-rate	SOC	Temperature (°C)
C0	Unaged	–	–
C2	2	0–10%	55
C4	4	0–10%	55
C7	~7	68% ± 7%	45

The aging experiments consisted of cycling the battery cells using the current profiles described above and conducting periodic capacity assessments until the measured cell capacity was degraded to 80% of the initial value. As an example of the results generated from the aforementioned tests, Fig. 5 reports the variation in the internal resistance and nominal capacity for the C2 cell sample.

Upon reaching the 80% residual capacity, the sample cells were completely discharged and then opened inside a glovebox filled with argon, while controlling the oxygen level at 88 ppm and dew point at −34 °C. The cells were unrolled and the anode and cathode strips were separated. Fig. 6 shows the layout of the unrolled electrodes strips, also illustrating the cylindrical cell described earlier along with the jelly roll of the electrodes and separator. In addition, the schematic in Fig. 6 shows the location of various sections along the length of the electrode strips. Each electrode strip was divided into six sections, where Section 1 corresponds to the region of electrodes near the outer circumference and Section 6 is near the center of the cylindrical cell. The NDP measurements described in the following section were conducted on electrode samples extracted from the Section 3 of all cells. As seen from the schematic in Fig. 6, Section 3 lies approximately at the middle of the electrode strip.

4.2. Results and discussion

The electrode samples extracted from the new and aged cells were mounted for the NDP experiments by safely loading and unloading them through the argon gas environment of the glove bag. The results from the NDP experiments were benchmarked against tests on the same samples previously conducted at the NIST-NDP facility. The energy spectrum of the 2727 keV ^{3}H particle was used to deduce the profile of the lithium concentration in the samples because of its two advantages over the corresponding energy spectrum of the 2055 keV ^{4}He particle. First, since the ^{3}H particle has a higher initial energy and less mass, the concentration profiles can be obtained to a greater depth in the sample. Second, the ^{3}H energy spectrum is not overlapped by the ^{4}He energy spectrum, but the ^{4}He energy spectrum is interfered with by the ^{3}H energy spectrum at low energies.

The samples described above were first studied at the NIST-NDP facility. The results of these measurements were then used in

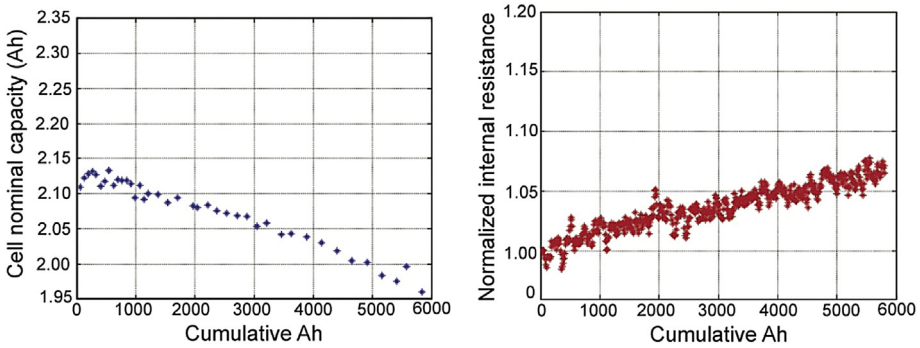

Fig. 5. Capacity fade (left) and internal resistance growth (right) for Li-ion cell aged according to protocol C2 [19–21].

comparing the performance of the modified OSU-NDP facility and benchmarking the system. Significant differences are present between the NIST-NDP facility and the OSU-NDP system described in this paper. The former uses "cold" neutrons with energy less than 5 meV, and has a single silicon surface barrier detector with an active depth of 75 μm and active area of detection of 150 mm^2. The detector was operated with a 30 V bias. The raw data is in the form of total number of counts in each channel of the detector. The concentration of ^6Li within the sample is determined by comparing the count rate observed from the sample with that of a well-characterized boron concentration standard, labeled as N6 [22]. The channel number is converted to energy using the energy calibration of the detector. The spectra are then smoothed with the Savitzky–Golay (SG) algorithm prior to representing the depth profiles [10]. The depth was defined using the methods discussed earlier in the NDP principle section.

The OSU-NDP facility is quite different from the NIST-NDP instrument, using 8 detectors and collecting data in list mode. Detectors in the OSU-NDP facility have energy resolutions between 18 and 26 keV, determined using a 5.48 MeV alpha particle source. 8 detectors are used to improve the charged particle detection efficiency of the instrument, allowing a greater fraction of particles to be detected despite having a neutron flux significantly lower than that of NIST's instrument. With the OSU reactor operating at 450 kW thermal power, neutron flux at the sample position is approximately 8.6×10^6 n cm^{-2} s, while NIST's reactor is capable of delivering a flux of 7.6×10^8 n cm^{-2} s. Histograms are generated offline for the data collected by each detector and channel summing is performed to add the spectra from all 8 detectors. Thereafter, data reduction is performed similar to the method described above and the depth profile is obtained. Fig. 7 shows the lithium concentration profiles measured on the samples at NIST-NDP (solid red line in the web version) and at the modified OSU-NDP facility (dotted blue line). Both experiments were conducted *ex-situ*, specifically on isolated samples of electrode materials under vacuum conditions.

The results show the clear advantage of the NDP technique for ex-situ analysis of Li-ion electrodes over other diagnostic techniques. Specifically, NDP allows for a non-destructive, quantitative evaluation of the lithium concentration distribution along the depth of the sample, limited to the region close to the exposed surface. The concentration measurements are spatially averaged over the area exposed to the incident beam. For the results discussed in this paper, the exposed area is approximately 0.8 cm^2. The porosity of the electrode materials is corrected by applying a lower density in SRIM calculation.

The behavior of the battery cells at the end of life is affected by the C-rate of the charge/discharge cycle of the battery and the SOC

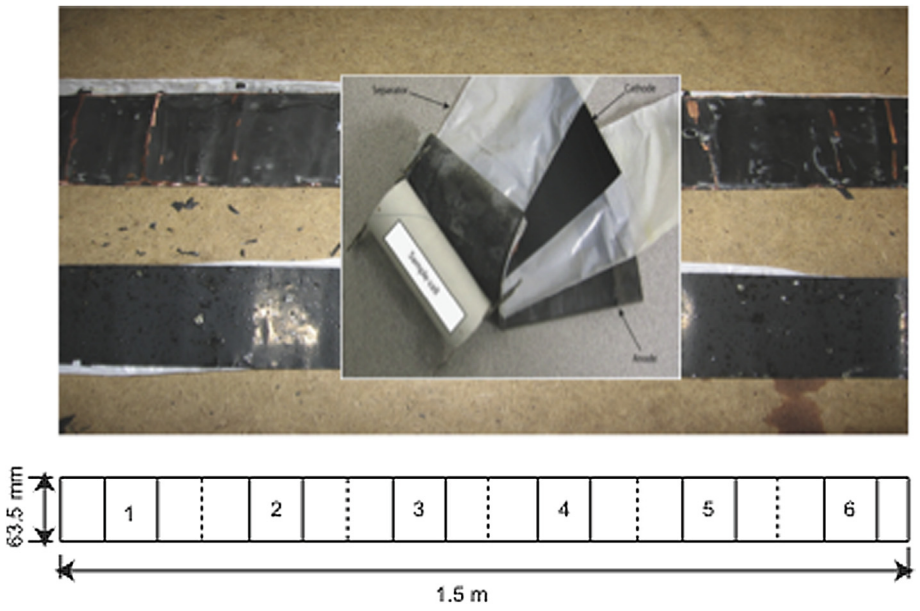

Fig. 6. Layout of the unrolled Li-ion cell and location of Section 3 within the electrode strips.

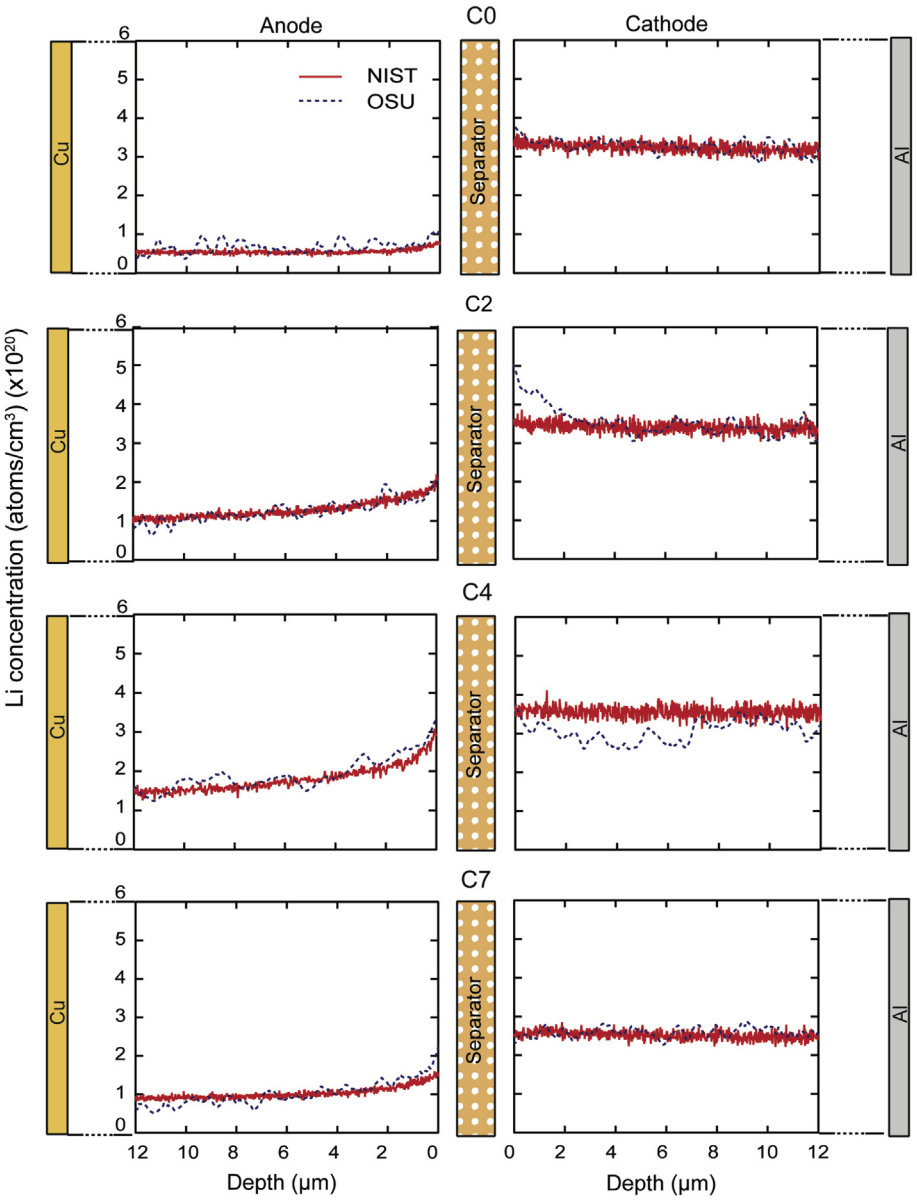

Fig. 7. Lithium concentration profiles in anode and cathode samples harvested from C0, C2, C4 and C7 cells. After the post-processing of the experimental data, the results from the NDP measurement are presented, showing the lithium concentration profile along the depth of the electrode samples for the various cells provided to this study.

at which the cell is cycled. In the case of the anode samples, the lithium concentration is maximum near the surface, and decays exponentially with the depth (thickness) of the sample. As expected for a sample harvested from completely discharged unaged cell (C0) (Fig. 7), the lithium concentration in the anode is significantly lower with very small amount of lithium buildup at the surface, while most of the lithium is concentrated in the cathode. The lithium concentration at the anode is higher on the surface for the aged batteries, and specifically increases with the C-rate. The buildup below the surface also extends to higher depths in cells cycled at higher C-rate. The lithium buildup on the anode surface from a cell cycled at higher SOC is less but increases with increasing C-rate. The lithium concentration profiles in the cathode show a uniform gradient, but the overall concentration decreases with higher C-rate and higher SOC.

Comparing the lithium concentration profiles measured at the NIST-NDP facility and the modified OSU-NDP facility, it is possible to observe a good match in terms of shape, concentration and depth values, with the exception of the C4 cathode sample. The mismatch of the concentration profiles in the C4 cathode sample can be considered as an outlier in the experiment. The concentration profiles were integrated along the depth of the sample in steps of 3 μm and the total concentration of lithium measured at OSU-NDP facility and NIST-NDP facility was compared (Table 3). Even though there is a significant difference in the count rate at the NIST-NDP facility and the OSU-NDP facility due to the difference in the available neutron flux, the eight solid state detectors at OSU allow a statistically significant number of counts to be collected in a reasonable amount of time. This helps to establish accurate concentration profiles along the depth of the samples. In the case of the anode, the error in measurement is in the range of 14–15%, except for the sample C7. For the cathode measurement, the error is least for sample C0 (<1%). The error in sample C2 is also <1%, except for the 0–3 μm depth due to the spurious peak in the measurement. The cathode samples C4 and C7 have the highest error, in the order of 7–8%.

Since the shape of the lithium concentration profiles is the same for all cases, the error is probably caused by a reduced exposure time, which prevents the acquisition of a significant distribution of energy counts. This issue could be mitigated by exposing the samples for longer time. Some of the cathode samples also present spurious peaks at the surface, which could be the result of the negative surface error attributed to error in aligning the zero depth with the first channel in the detector.

Nagpure et al. [10] have attributed the observed nature of the lithium concentration in anode and cathode samples to the coarsening of the $LiFePO_4$ particles during the aging of the cells. The effects of coarsening of the particles is the change in the effective surface area affecting the rate of the reaction, and change in the ionic path lengths affecting the diffusion kinetics of the lithium ions during charging and discharging cycles. As a result, the net uptake of lithium during the discharging processes is low especially at higher C-rate. During each charge cycle lithium diffuses out of the $LiFePO_4$, and phase change occurs from $LiFePO_4$ to $FePO_4$. In the discharge cycle the lithium diffuses back in the host $FePO_4$ particle, and the phase changes from $FePO_4$ to $LiFePO_4$. During the early life of the battery the phase change from $LiFePO_4$ to $FePO_4$ and back to $LiFePO_4$ might be complete, but as the particle size increases due to coarsening, the diffusion length changes, and this will affect the phase change. The incomplete phase change continues to occur in subsequent cycles while the particle size tends to increase. Thus the lithium retaining capacity of the particle drops in each subsequent cycle. The loss of active lithium in the cathode is directly related to the drop in capacity of the battery while the increase in the particle size and the subsequent increase in the diffusion length are directly related to the rate capabilities of the battery.

Table 3
Comparison of total lithium concentration at various depths measured at NIST-NDP and OSU-NDP facility.

Depth (μm)	NIST (atoms)	OSU (atoms)	Percent error
Anode			
C0			
0–3	1.25E+16	1.44E+16	14.64
0–6	2.50E+16	2.85E+16	14.01
0–9	3.75E+16	4.27E+16	13.80
0–12	5.00E+16	5.68E+16	13.70
C2			
0–3	2.51E+16	2.26E+16	−9.93
0–6	5.01E+16	4.49E+16	−10.42
0–9	7.52E+16	6.72E+16	−10.58
0–12	1.00E+17	8.95E+16	−10.66
C4			
0–3	3.12E+16	3.60E+16	15.23
0–6	6.23E+16	7.14E+16	14.60
0–9	9.33E+16	1.07E+17	14.39
0–12	1.24E+17	1.42E+17	14.28
C7			
0–3	2.12E+16	1.69E+16	−20.06
0–6	4.23E+16	3.36E+16	−20.50
0–9	6.33E+16	5.03E+16	−20.65
0–12	8.44E+16	6.69E+16	−20.72
Cathode			
C0			
0–3	7.40E+16	7.36E+16	−0.52
0–6	1.48E+17	1.47E+17	−0.46
0–9	2.21E+17	2.20E+17	−0.44
0–12	2.95E+17	2.94E+17	−0.43
C2			
0–3	7.91E+16	6.55E+16	−17.14
0–6	1.58E+17	1.57E+17	−0.58
0–9	2.37E+17	2.35E+17	−0.56
0–12	3.15E+17	3.14E+17	−0.55
C4			
0–3	8.36E+16	7.44E+16	−10.98
0–6	1.67E+17	1.49E+17	−10.92
0–9	2.50E+17	2.23E+17	−10.91
0–12	3.33E+17	2.97E+17	−10.90
C7			
0–3	5.79E+16	6.22E+16	7.41
0–6	1.15E+17	1.24E+17	7.48
0–9	1.73E+17	1.86E+17	7.50
0–12	2.31E+17	2.48E+17	7.51

4.3. Feasibility study for in-situ NDP

Following the benchmarking of the OSU-NDP system, a preliminary study was conducted to verify the feasibility of in-situ NDP, specifically conducting a measurement of the lithium concentration profile for electrode samples under an inert gas atmosphere at ambient pressure conditions.

For this test, helium was chosen as the inert gas, due to its transparency to neutrons. In order to assess the impact of He on an NDP measurement, a stopping range calculation was performed using the Stopping Range of Ions in Matter (SRIM) code [14]. The results of the simulations for He gas at 25 °C, and 1 atm are shown in Fig. 8.

According to the simulations, the maximum range of 2727 keV ^3H particles in He is greater than 126 mm, which is the distance between the surface of the electrode sample and the detectors. Similarly, the maximum range of 2100 keV ^3H particles (i.e., the lowest energy of ^3H particles before 2055 keV ^4He particle interference begins) is also greater than 126 mm, indicating that the entire useful range of ^3H particles could potentially be used for analysis in the presence of a He atmosphere.

Since the ^3H particles from the sample spectra can be detected in a He gas atmosphere, this inert gas was chosen to augment the instrument design, allowing the OSU-NDP system to conduct in-situ NDP studies of Li-ion electrodes. The design was tested with an experiment to measure the lithium concentration profile on the anode sample harvested from the C4 cell. (The readers should note that this is the same sample used in the earlier part of the work, and the lithium concentration profile of this sample measured at the NIST and OSU-NDP facilities was reported in Fig. 6.) The lithium concentration profile of this sample measured at the OSU-NDP facility in vacuum is considered as the baseline for comparison and data analysis.

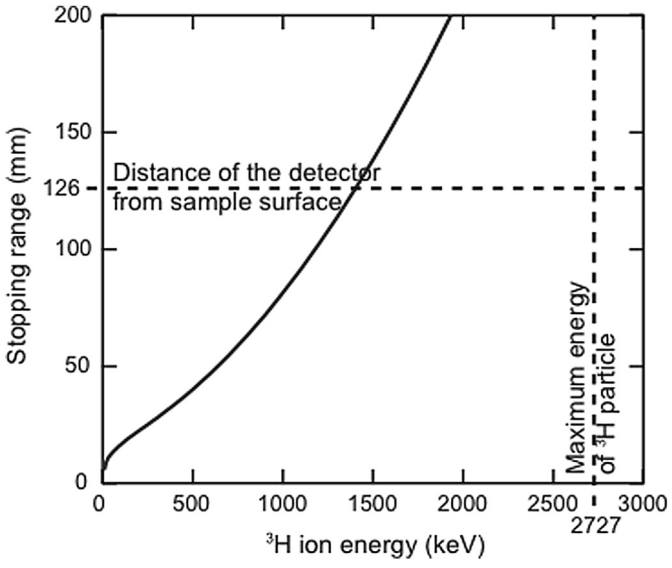

Fig. 8. Stopping range of ^3H particle traveling through 12.6 cm layer of He gas layer at 1 atm.

The C4 anode sample was loaded into the NDP chamber filled with argon gas, following the same protocol established earlier to handle the air-sensitive samples. Once the NDP chamber was evacuated to ensure that there are no traces of argon gas, the chamber was back filled with Helium gas to a pressure of nearly 1atm. The NDP measurement was then conducted by irradiating the sample with neutrons for an exposure of approximately 20 min.

The resulting profile (dashed-dot line) is shown in Fig. 9 and compared to the profiles obtained in vacuum, depicted in Fig. 6. The profile was calculated using the energy of the ^{3}H particle and applying the same procedure for data reduction as discussed at the beginning of this section.

Since the ^{3}H particle loses energy while travelling from the sample surface through the He gas atmosphere, the spectrum captured at the detectors is shifted to lower energies. This shift in the energy spectrum is accounted for by aligning the ^{3}H energy peak at the surface of the sample (zero depth) with the similar peak in the spectrum from the data measured in the vacuum.

The shape of the profile measured in the He gas atmosphere differs from the results obtained by measuring in vacuum. In particular, the profile starts to deviate after 3 μm, and continues to diverge beyond 6 μm. Also, it is observed that the peak in the profile at the surface is lower than the earlier reported peak measured in vacuum. Considerable peak broadening was observed in the measured data at the surface of the sample, which is to be expected due to increased straggling as ^{3}H particles traverse the He gas atmosphere. The number of counts for the profile measured in He gas atmosphere was an order of magnitude lower than the profile measured in vacuum. The difference in the counts was more significant for lower energies, suggesting that if the collection time is increased considerably, the effects of deviation in the profile and the peak broadening should be minimized.

Based on the initial experimental results, the impact of the He gas pressure and concentration on the accuracy of the measurements was evaluated with simulations, through the Transport of Ions in Matter (TRIM) software [14]. TRIM is based on a Monte Carlo simulation that calculates the interactions of energetic ions with amorphous targets. For this analysis, simulations were performed at the two energy levels for ^{3}H particles at different pressures, ranging from 0.8 atm to 1 atm. The objective was to observe the energy shift under a range of pressures higher than the vapor pressure of the electrolyte. The simulations are run for the ion counts obtained from the raw data collected at the NIST-NDP facility.

In Fig. 10a, the energy distribution of ^{3}H particle at 2727 keV after passing through a 126 mm thick He gas layer at different pressures is shown. The energy shift is maximum at 1 atm. Also, the normalized counts are lower in the case of 1 atm and increase at lower pressures. Similarly, Fig. 10b shows the trends in energy shift and normalized counts observed with pressure for ^{3}H particle at 2103 keV. If the measurements are conducted at higher He gas pressure, then the count time must be longer to compensate for the statistical error due to fewer total counts. Also, at higher pressure the depth to which the lithium concentration can be obtained will decrease as the energy at 2103 keV is close to 1111 keV which is very close to the background signal of the instrument. As the He gas pressure decreases, the count rate increases and the depth range also increases.

Summarizing, the simulation results suggest that improved accuracy can be achieved by conducting the in-situ measurements at pressures just above the vapor pressure of the electrolyte. At these

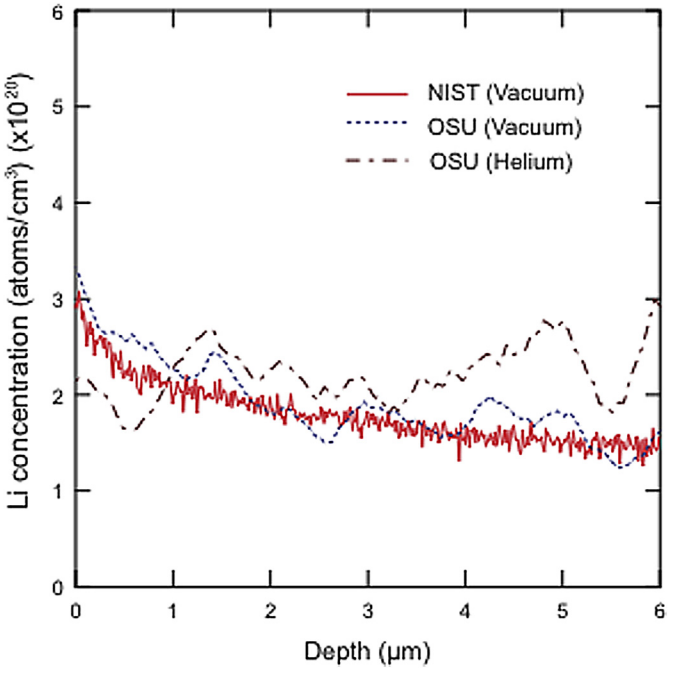

Fig. 9. Li concentration profile in anode sample harvested from C4 cell measured in vacuum and in He gas atmosphere at 1 atm.

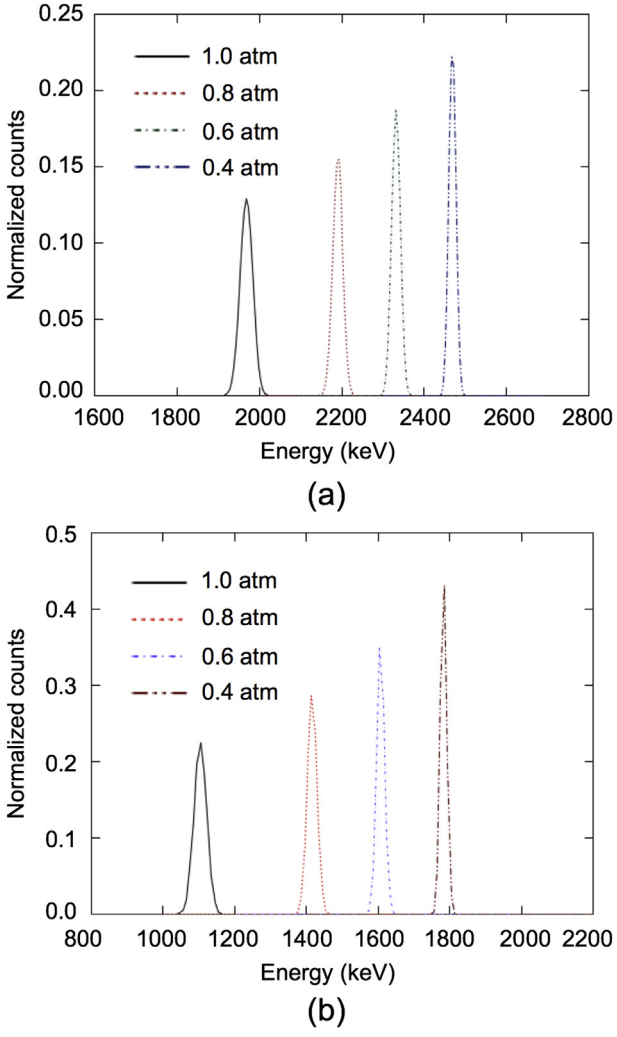

Fig. 10. TRIM simulations of (a) 2727 keV and (b) 2103 keV ^{3}H particle traveling through 12.6 cm layer of He gas layer at various pressures.

conditions, the count time can be optimized to achieve the desired accuracy in the measurement.

5. Conclusion

This paper describes an NDP experimental setup designed for measuring the lithium concentration profiles in the near-surface region of the electrodes of commercial Li-ion batteries and, largely, of air-sensitive materials. The paper describes a NDP facility capable of handling and measuring the concentration profiles in air-sensitive Li-ion battery samples. An intermediate inert gas chamber was built to load and unload the samples to the NDP chamber. The lithium concentration profiles measured agree well with the profiles previously collected at NIST on the same samples. Furthermore, NDP was conducted in a He gas-filled environment to demonstrate the possibility of in-situ measurement of lithium concentration during the operation of the Li-ion cell containing a liquid electrolyte. While the results are promising, it indicated that the pressure of the He gas should be optimized with the trade off between vapor pressure and the energy loss of the charged particles from Li and incident neutron reaction.

Acknowledgment

The authors would like to thank Jie Qiu and The Ohio State University Research Reactor staff for their help in conducting the experiments.

This material is based upon work supported by the Department of Energy under Award Number DE-PI0000012. This report was prepared as an account of work sponsored by an agency of the United States Government. Neither the United States Government nor any agency thereof, nor any of their employees, makes any warranty, express or implied, or assumes any legal liability or responsibility for the accuracy, completeness, or usefulness of any information, apparatus, product, or process disclosed, or represents that its use would not infringe privately owned rights. Reference herein to any specific commercial product, process, or service by trade name, trademark, manufacturer, or otherwise does not necessarily constitute or imply its endorsement, recommendation, or favoring by the United States Government or any agency thereof. The views and opinions of authors expressed herein do not necessarily state or reflect those of the United States Government or any agency thereof.

References

[1] V. Etacheri, R. Marom, R. Elazari, G. Salitra, D. Aurbach, Energy Environ. Sci. 4 (2011) 3243–3262.
[2] S.C. Nagpure, S.S. Babu, B. Bhushan, A. Kumar, R. Mishra, W. Windl, L. Kovarik, M. Mills, Acta Mater. 59 (2011) 6917–6926.
[3] J. Vetter, P. Novák, M.R. Wagner, C. Veit, K.C. Möller, J.O. Besenhard, M. Winter, M. Wohlfahrt-Mehrens, C. Vogler, A. Hammouche, J. Power Sources 147 (2005) 269–281.
[4] H. Wang, R.G. Downing, J.A. Dura, D.S. Hussey, in: K. Page, et al. (Eds.), Polymers for Energy Storage and Delivery: Polyelectrolytes for Batteries and Fuel Cells, ACS Symposium Series, American Chemical Society, Washington, DC, 2012, pp. 91–106 (Chapter 6).
[5] J.F. Ziegler, G.W. Cole, J.E.E. Baglin, J. Appl. Phys. 43 (1972) 3809–3815.
[6] R.G. Downing, R.F. Fleming, J.K. Langland, D.H. Vincent, Nucl. Instrum. Methods 218 (1983) 47–51.
[7] R.G. Downing, G.P. Lamaze, J.K. Langland, S.T. Hwang, J. Res. Natl. Inst. Stand. Technol. 98 (1993) 109–126.
[8] J.P. Biersack, D. Fink, Nucl. Instrum. Methods B 149 (1978) 93–97.
[9] S. Whitney, S.R. Biegalski, Y.H. Huang, J.B. Goodenough, J. Electrochem. Soc. 156 (2009) A886–A890.
[10] S.C. Nagpure, R.G. Downing, B. Bhushan, S.S. Babu, L. Cao, Electrochim. Acta 56 (2011) 4735–4743.
[11] S.C. Nagpure, R.G. Downing, B. Bhushan, Scripta Mater. 67 (2012) 669–672.
[12] J.F.M. Oudenhoven, F. Labohm, M. Mulder, R.A.H. Niessen, F.M. Mulder, P.H.L. Notten, Adv. Mater. 23 (2011) 4103–4106.
[13] X.H. Liu, J.Y. Huang, Energy Environ. Sci. 4 (2011) 3844–3860.
[14] J.F. Ziegler, M.D. Ziegler, J.P. Biersack, Nucl. Instrum. Methods B 268 (2010) 1818–1823.
[15] P.L. Mulligan, L.R. Cao, D. Turkoglu, Rev. Sci. Instrum. 83 (2012) 073303–073308.
[16] S. Franger, Le. F. Cras, C. Bourbon, C. Benoit, P. Soudan, J. Santos-Penã, in: S.G. Pandalai (Ed.), Recent Research Developments in Electrochemistry, vol. 8, Transworld Research Network, Kerala, 2005, pp. 225–256.
[17] Anonymous, USABC Battery Test Manual for Plug-in Hybrid Electric Vehicles, USABC, Southfield, MI, 2008.
[18] Anonymous, USABC Requirements of End of Life Energy Storage Systems for PHEVs, USABC, Southfield, MI, 2006. Available from: www.uscar.org/guest/view_team.php?teams_id=12.
[19] P. Spagnol, S. Onori, N. Madella, Y. Guezennec, J. Neal, in: 6th IFAC Symposium Advances in Automotive Control, 2010, pp. 186–191. Schwabing, Germany.
[20] A. Di Filippi, S. Stockar, S. Onori, M. Canova, Y. Guezennec, in: Proceedings of the 2010 IEEE Vehicle Power and Propulsion Conference, IEEE, Lille, France, 2010, pp. 1–6.
[21] S. Onori, P. Spagnol, V. Marano, Y. Guezennec, G. Rizzoni, Int. J. Power Elect. 4 (2012) 302–319.
[22] D.M. Gilliam, G.P. Lamaze, M.S. Dewey, G.L. Greene, Nucl. Instrum. Methods Phys. Res. Sect. A Accel. Spectrom. Dect. Assoc. Equip. 334 (1993) 149–153.